Assessment of Ionic Liquids as H_2S Physical Absorbents by Thermodynamic and Kinetic Analysis based on Process Simulation

Rubén Santiago, Jesús Lemus*, Ana Xiao Outomuro, Jorge Bedia and José Palomar

Chemical Engineering Department. Universidad Autónoma de Madrid. 28049 Madrid. Spain.

*Corresponding author. E-mail: jesus.lemus@uam.es

Keywords: H_2S; Absorption; COSMO-RS; Ionic Liquids; Aspen Plus

Abstract

A comprehensive evaluation of ionic liquids (ILs) as potential H_2S absorbents was performed using both molecular and process simulation. First, the Conductor-like-Screening MOdel for Real Solvents (COSMO-RS method) was applied to select promising ILs absorbents and to understand the H_2S gas solubility from a molecular point of view. The ILs screening more than 700 ionic combinations determines that H_2S physical absorption is mainly controlled by the hydrogen-bond acceptor capacity of the anion, due to the easily hydrogen bond formation when mixed with the acidic solute. Based on molecular simulation analysis, 6 ILs of different nature were evaluated in a typical industrial packed absorption column using COSMO-based/Aspen Plus methodology. Equilibrium based simulations demonstrated higher H_2S separation efficiency *(i.e.* lower solvent expenses and smaller equipment sizes) when increasing H_2S absorption capacity of the IL solvent. In contrast, rigorous process simulation analysis (including kinetic equations) reveals a strong mass transfer kinetic control in the H_2S absorption in commercial packed column, which severely limits the maximum H_2S absorption given by thermodynamics. As a result, ILs that present the best performance in the thermodynamic aspect, become worse for the operation. In fact, it was found that H_2S recovery at given operating conditions increases when decreasing the viscosity of IL, being 1-ethyl-3-methylimidazolium dicyanamide, the one that presents the best absorbent performance, requiring the lowest operating temperatures and liquid volume flows. Lastly, the absorption operation was designed to achieve fixed H_2S recovery using different liquid/gas feed ratios, resulting in column heights and diameters inside the

typical range marked by heuristic rules for usual industrial packed columns. In sum, current prospective study based on COSMO-RS and Aspen Plus have been proved as a useful tool to analyze the potential industrial application of ILs in the H_2S capture and to select the most adequate ILs, before starting with experimental tests, highly demanding in cost and time.

Introduction

In recent years, natural gas has become one of the most promising alternatives to the traditional and pollutant energy sources due to its cleanliness [1]. The active component in natural gas is methane (CH_4), but it usually contains undesired impurities such as carbon dioxide (CO_2) and hydrogen sulfide (H_2S) [2]. H_2S is an extremely toxic and corrosive gas that can cause several diseases and even the potential dead in enough concentrations [3]. H_2S is one of the responsible compounds of the well-known "acid rain" when it is oxidized to SO_2, causing extremely negative effects to the different ecosystems [4]. For all these reasons, the complete removal of H_2S from natural gas is required not only for a safety transport, but also for its correct utilization. Furthermore, the removal of this acid gas increases the calorific value of the natural gas [5].

Some technologies are available for H_2S treatment. Starting with the adsorption operation, some adsorbents such as silica gel, active carbon and zeolites are traditionally used. Specially, high specific surface zeolites demonstrated a great efficiency with high H_2S selectivity, and great stability until high temperatures [6]. However, the main disadvantage of this technology is the high energy demanding in the regeneration operation that hinders the application of this technology [7]. The technology most widely studied is H_2S absorption. In fact, a huge number of solvent-based processes were analyzed to remove this acid gas [8]. The separation has been accomplished by using chemical and/or physical absorption processes. Starting with the former, the most typical absorbents used are the aqueous organic amine solutions [9, 10]. They present high absorption capacities at low partial pressures, but they become less effective when the absorbent is reaching the saturation [8]. These absorbents show some disadvantages in their use, such as the high energy consumption due to the heat requirements to release the H_2S from the solvent and their high losses because of their high volatility [11]. In addition, the presence of CO_2 in the streams, results in competitive absorption, being the H_2S separation capacity reduced [11]. In the case of physical absorption, it presents some

advantages when compared with the chemical one, such as the easy regeneration at lower temperatures. Some physical absorbents are methanol, dimethylether, and morpholine derivatives, which are employed in commercial processes: Rectisol®, Selexol® and Morphysorb®, respectively [12]. However, Rectisol® presents a high volatility and low H_2S selectivity when CO_2 is present on the stream to treat. Selexol® presents lower vapor pressure than traditional solvents usually employed, but it presents high viscosity, which will result in low mass transfer kinetics. Morphysorb® presents high volatility, which will make more difficult the regeneration stage. [13]. These advantageous properties are the high and tunable solvent capacity, negligible volatility, non-flammability, low corrosivity and relatively high chemical and thermal stability [13, 14]. Furthermore, the possibility of customizing the cation and/or the anion for specific tasks made them considered as "designer solvents" [15]. The introduction of the ILs to physically absorb H_2S has attracted a great scientific community interest in recent years. Several works studying the H_2S solubility in different ILs physical absorbents were reported [16-20]. In that way, a pioneer work by Pomelli *et al*. [21] reported an experimental and theoretical study on solubility using different nature based ILs, concluding the importance of hydrogen bond interactions between the anion and the acid gas showing less importance the cation selection. This finding was confirmed later by Aparicio *et al.* [22] and Sakhaeinia *et al.* [23]. In parallel, several studies using COSMO-RS method performed computational screenings to select ILs with high H_2S gas solubility, in order to minimize the high cost and time demanding experimental tests [24-26].

In recent years, we have followed a multiscale research strategy, that integrates molecular and process simulations, to design new gas separation process based on ILs [27-29], successfully applied to the capture of CO_2 [30-33], NH_3 [34], toluene [35], acetylene [27] and other volatiles organic compounds [36-38]. This computational methodology can be applied to preliminary evaluate the technical viability of novel gas absorption process using ILs prior to experimental tests. For this purpose, the free ILUAM database [28] was recently developed to include 100 common ILs as compounds in Aspen Plus/Hysys software, in order to easily model individual operation units and complete separation processes based on ILs. This COSMO-based/Aspen Plus approach allows considering, simultaneously, thermodynamic, kinetic, technical, energetic and economic criteria in the selection of the most adequate IL absorbent. In addition, operating conditions, equipment

design and process configuration can be optimized in order to promote the technical and economic viability of the new separation process based on ILs [30, 31, 39, 40].

The main aim of this work is to evaluate and select adequate ILs for the H_2S absorption by means of the COSMO-based/Aspen Plus methodology. First, molecular simulation was used to select ILs with favorable thermodynamic properties for H_2S capture. For this purpose, a COSMO–RS screening of Henry's law constants of H_2S in more than 700 ILs was carried out to determine the more favorable cation-combination for H_2S absorption, selecting a sample of ILs with favorable H_2S absorbent properties. Then, the excess enthalpies of H_2S-IL binary mixtures were analyzed in terms of the solute-solvent intermolecular interactions, in order to obtain deeper insight of H_2S physical absorption phenomena in IL. Finally, process simulation with Aspen Plus process simulator was accomplished to describe the H_2S capture by IL in packing column at industrial scale. An equilibrium-based model was preliminary applied to analyze the role of thermodynamics in H_2S absorption operation, including the influence of the operating pressure, gas/liquid ratio (L/G) and number of column stages (N) on the H_2S recovery. Then, the potential kinetic control on the H_2S absorption process at different operating temperatures was analyzed by using rigorous rate-based column model. Finally, the sizing of the absorption column was performed for the best IL in order to achieve 95% H_2S recovery at different L/G ratios, obtaining in each case the required height and diameter of the packed column and comparing the results with the heuristic industrial parameters.

Methodology

COSMO-RS calculations

The first stage in COSMO-RS calculations is to create the *.cosmo files of the ILs for their use in COSMOtherm software. For this, the optimization of the compounds was performed at BP86/TZVP computational level by using Turbomole 7.0 software. ILs are defined using the molecular model of independent counter ions ($C + A$) in which the cation and the anion are optimized separately. These optimizations were carried out taking the compounds to the structure of minimum energy, with the solvent effect through the COSMO continuum solvation method. Once the optimization was finished, the polarized charge distribution of the compounds is obtained by a COSMO single point calculation, saving it into *.cosmo files. Then, the COSMO-RS calculations were performed using the COSMOtherm program package (version C30_1704) and its parametrization

BP_TZVP_C30_1701. The charge distributions of both H_2S, as pure solute, and ILs, as absorbents, can be easily visualized in σ-profile and σ-potential. In addition, vapor pressure calculation of H_2S at different temperatures was performed. In the case of the solute-solvent mixtures, Henry's law constants of H_2S in ILs and detailed contributions to excess enthalpies in equimolar mixtures were calculated as well. First, Henry's law constants (K_H) are calculated as follows:

$$K_H = \gamma_i^{\infty} \cdot p_0^{vap} \quad [1]$$

where K_H is calculated as the product of γ_i^{∞} , which is the activity coefficient of the solute at infinite dilution in the IL (calculated by COSMOtherm) and p_0^{vap} , which is the vapor pressure of the pure gas, estimated by Antoine equation (experimental data from reference [41]).

Second, the excess enthalpy of an equimolar mixture (H^E) is calculated by COSMOtherm following the next expression:

$$H^E = H^E(MF) + H^E(HB) + H^E(vdW) \quad [2]$$

Where $H^E(MF)$ is the energy contribution associated to Misfit forces; $H^E(MF)$ is that attributed to the hydrogen bonding and $H^E(vdW)$ is the one ascribed to Van der Waals forces.

Process simulation details

ILs were directly used from ILUAM database [28], which includes information and parameters of 100 commercial ILs for its application in Aspen Process simulators. COSMOSAC property package was selected for the thermodynamic calculations. In the case of the conventional gaseous compounds used in this work, which are N_2, CH_4, H_2S, and CO_2, they were loaded from Aspen Plus Database including two parameters for the complete definition of COSMOSAC property package. In this sense, the σ-profile and COSMO volume of the gaseous compounds were first calculated by using COSMOtherm software and then introduced to Aspen Plus process simulator. The use of COSMOSAC property package lets the user select the model that better fits to the system. Therefore, the user can select between: (i) the original COSMO-SAC model proposed by Lin and Sandler [42] (denoted as COSMOSAC 1); (ii) the original COSMO-RS model developed by Klamt [43] (COSMOSAC 2); and (iii) a modification of the Lin and Sandler model performed by P. Mathias *et. al* [44] (COSMOSAC 3). In the present work, the three

models were used for selecting the one that best fits to the experimental data. Mean relative error were calculated by eq. 3 using the experimental and calculated gas-liquid equilibria (GLE) data 30%. COSMOSAC 1 property model shows the best fit to the experimental data, with errors lower than 16%, which can be considered an admissible error on initial stages of conceptual engineering [39]. Therefore, COSMOSAC 1 is selected as the property model for next stages of the work.

$$Mean\ relative\ error\ (\%) = \frac{1}{N_{point}} \sum \frac{|x_{calculated} - x_{experimental}|}{x_{calculated}} \cdot 100 \qquad [3]$$

The RADFRAC model implemented as default in Aspen Plus v9.0 was used to model the H_2S absorption column. To accomplish this, two operation modes of RADFRAC model were used: *Equilibrium* mode, in which only the thermodynamic equilibrium is considered, and *Rate-Based* mode, in which also the mass transfer kinetics is taken into account. For *Rate-Based* calculations, a fractional capacity of 65% was fixed to ensure a similar fluid dynamic behavior. A packing type *Raschig Rings* with a diameter of 76.2 mm was selected following the heuristic rules for maintaining a *D/d* ratio around 20 [45].

The inlet gas feed presents the composition summarized in Table 1, accordingly to Faramawy *et. al*. work, for typical acid gas natural streams of industrial plants [2].

Table 1. Inlet gas feed general characteristics.

Stream characteristics		**Value**	
P, atm		0.98	
T, ºC		25	
Total Molar Flow, kmol/h		1301	
Total Mass Flow, ton/h		22.5	
Component	***MW*, kg/kmol**	y_i	**Flow, kmol/h**
CH_4	16	0.940	1222.9
CO_2	44	0.025	32.5
N_2	14	0.015	19.5
H_2S	34	0.020	26.1

Different simulation cases were performed for studying both the thermodynamics and the kinetics of the H_2S absorption operation using ILs: *Case 1):* The *Equilibrium* mode of RADFRAC column was used for studying the influence of the *L/G* ratio at two given

pressures in the H_2S recovery in different ILs. *Case 2):* Once again using the equilibrium column, the number of stages was varied for obtaining 99% of recovery at a fixed *L/G* ratio. *Case 3):* The H_2S recoveries as a function of the temperature are estimated for the selected ILs using *Equilibrium* and *Rate-Based* mode in RADFRAC column (1 m of height). *Case 4):* Comparison of *L/G* ratio for reaching a 95% H_2S recovery at different temperatures between *Equilibrium* and *Rate-Based* mode of different ILs. All the used conditions for each case are summarized in Table 2. Last, the column design (height and diameter) was accomplished for the best case taking into account heuristic rules. In this sense, the enough height for reaching a 95% H_2S recovery, and the diameter needed for a fractional approach to maximum capacity of 65% as a function of the *L/G* ratio.

Table 2. Conditions of the different cases of study.

Case	**1**	**2**	**3**	**4**
Mode	EQ	EQ	EQ/RB	EQ/RB
Pressure, atm	3-30	30	30	30
***T*, ºC**	25	25	0-200	0-100
***L/G*, kg/kg**	0-200	-	30	-
H_2S recov, %	-	99	-	95
Number of Stages	2	2-10	5	5

Results

Molecular simulation

COSMO-RS methodology allows predicting the thermodynamic properties of solute-IL systems and analyzing the intermolecular interactions governing the mixture behavior. This is due to the quantification of the interaction energy between the surfaces by means of the polarized charge distribution (σ). This charge distribution can be summarized in a histogram named σ-profile that permits a simple analysis of the chemical nature of the compounds involved. Next, COSMO-RS introduces an additional tool called σ-potential in which the charge density concept is introduced. This is defined as the chemical potential of a surface unit with a polarized charge distribution in a solvent, and allows

analyzing the intermolecular interactions between the compound and its environment [46]. In this sense, Figure 1 shows the σ-profile and σ-potential results of the solute studied (H_2S). It is important to remark the three different regions in which the histograms are divided. The first one that includes the range of polarities $\sigma < -0.0082$ e/Å^2 is referred to the hydrogen bond donor groups, the second one ($-0.0082 < \sigma > +0.0082$ e/Å^2) includes the non-polar region and the last one $\sigma > +0.0082$ e/Å^2 associated to hydrogen bond acceptor groups. The σ-profile of H_2S presents a peak at the negative region (hydrogen bond donor group), in agreement with the weak H_2S acidity. On the other hand, attending to the σ-potential (Figure 1B), it is observed that H_2S presents attractive interactions with non-polar compounds and polar compounds presenting weak hydrogen bond acceptor groups, as seen on the exothermic behavior near the cut-off region.

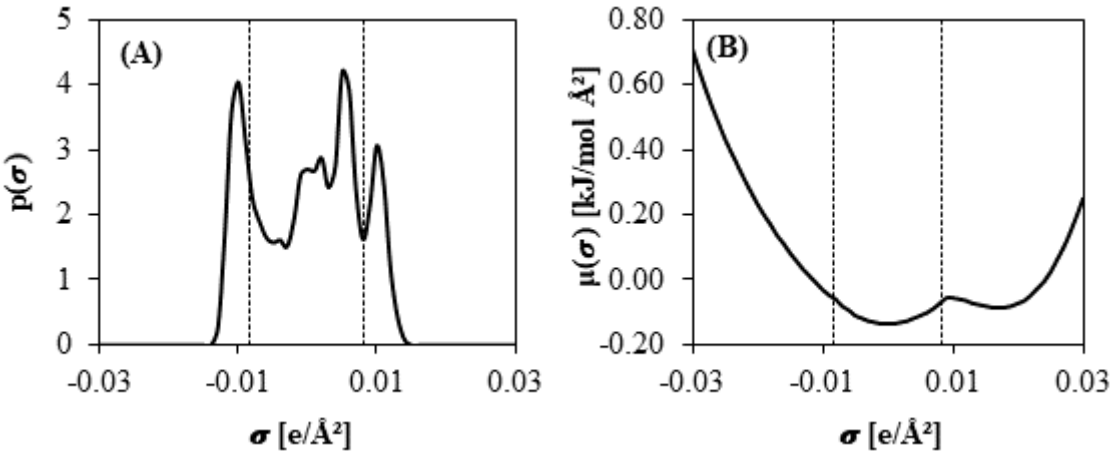

Figure 1: **(A)** σ-profile and **(B)** σ-potential of pure H_2S

The next stage of molecular simulation is to select ILs among a huge database. A widely used key parameter for the selection of ILs as absorbent -attending to thermodynamic criteria- is the Henry's law constant of the gas solute in the IL. Following the equation (1), COSMO-RS method calculates K_H by means of the activity coefficient of the solute at infinite dilution in the mixture and the vapor pressure of the pure solute. In current COSMO-RS calculations, the experimental vapor pressure was included in the software by means of Andrade equation parameters (A= 4.52887; B= 958.587 and C= -0.539 units of bar). For validation purposes, Figure 2 shows the experimental K_H *vs* the calculated K_H

for several different solutes in ILs, using the [*C*+*A*] model to describe the IL component in COSMO-RS simulations, following the methodology of previous works [27, 32, 36]. It is important to remark that the experimental K_H values were collected from Gonzalez-Miquel *et. al.* work [36] (more information in Table S1 of Supporting Information). As can be seen, the statistical parameters (slope = 0.99 and square correlation coefficient R^2 = 0.98) show the good predictability of COSMO-RS approach used in this work, including the available data for H_2S-IL systems (Table S1 of Supporting Information collects all the data and references presented in Figure 2).

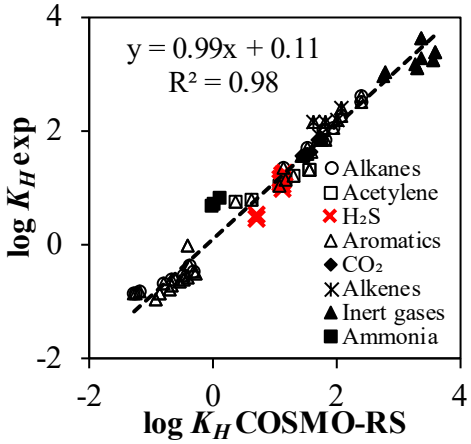

Figure 2: Henry's law constant prediction validation using [*C*+*A*] model and experimental vapor pressure of solutes using COSMO-RS calculations at near room temperature

Then, a complete Henry's law constant screening among more than 20 combinations cation-anion (>700 ILs) was performed for selecting ILs with potential properties for H_2S absorption. Remarkably different nature cations and anions were used for the screening (see Table S2 in the Supplementary Material for the nomenclature of the ILs used). Figure 3 presents the results of predicted K_H of H_2S in the different cation-anion combinations. It is important to remark that, following the equation (1), low K_H values are traduced into high solubility values in molar terms. Therefore, we search combinations cation-anion that present the lowest K_H values. Analyzing the Figure 3, it is observed that the K_H values for several ILs are lower than 2 bar, indicating a higher H_2S solubility than that of CO_2 in ILs [33] and in the order of that of similar to NH_3 in ILs [47]; *i.e*, we found favorable cation-anion combinations for the H_2S absorption in comparison to other solutes [36]. Attending to COSMO-RS predictions depicted in Figure 3, the selection of both anion and cation has significant influence on the H_2S absorption capacity of the IL [40], obtaining higher values with those ILs composed by

anion with basic character ($[MePO_3]^-$, $[(Me)_2PO_4]^-$, $[MeSO_3]^-$ …) and aprotic cations with non-polar character (phosphonium, ammonium …).

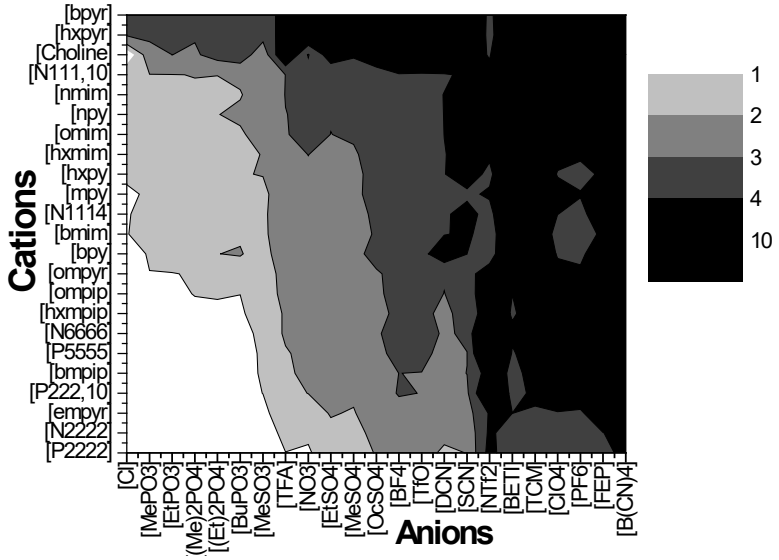

Figure 3: Henry's law constants screening (bar) of H_2S in 529 ILs at 25 ºC

To analyze the possible relationship between the H_2S solubility in ILs and the excess enthalpy of H_2S-IL mixtures, COSMO-RS method was applied to calculate the H^E values of the H_2S-IL mixtures at H_2S concentrations corresponding to the solubility data in ILs. Figure 4 relates the predicted K_H values of H_2S in IL to the excess enthalpy of the equimolar solute-solvent mixtures at 25 ºC and 1 atm. As can be seen, the gas solubility increases (lower K_H) in more exothermic mixtures, indicating that the favorable intermolecular interactions between H_2S and IL determine the absorption process, in good agreement with the previously observed for CO_2, NH_3, VOCs, etc. capture [27, 30, 32, 34, 36, 40, 47]. As can be seen, from molecular simulations, we can select ILs that present higher exothermic mixtures and lower K_H values than common ILs widely used in bibliography [16-18, 48, 49].

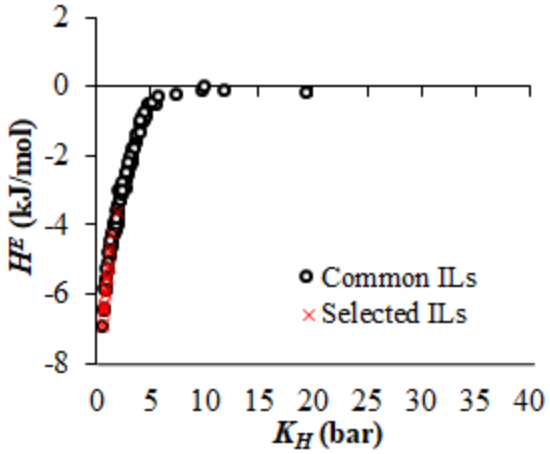

Figure 4: Molar Excess Enthalpies (H^E) *vs* Henry's law constants (K_H) of equimolar H_2S-ILs mixtures at 25 ºC

In order to obtain more insights in the intermolecular contributions to the H_2S absorption, different COSMO-RS analysis can be performed. In this sense, we first analyze the effect of the anion nature on H_2S-IL mixture behavior. It is going to be analyzed different chemical nature effects of ILs. First, Figure 5 presents the calculated H^E and K_H for ILs series of common $[emim]^+$ cation and different anions. As can be seen, remarkably enhanced H_2S gas solubility can be obtained by the proper selection of the anion. Thus, ILs with strong hydrogen-bond acceptor groups promote favorable solute-solvent intermolecular interactions that increase the gas solubility. On the contrary, anion with delocalized charge, such as $[PF_6]^-$, is not able to form local HB interactions with the solute, and as result, low solubility of H_2S in the ILs formed by this anion is expected. It was demonstrated that the anion contributes majority to the H_2S physical absorption and the importance of selecting anions that present basic character.

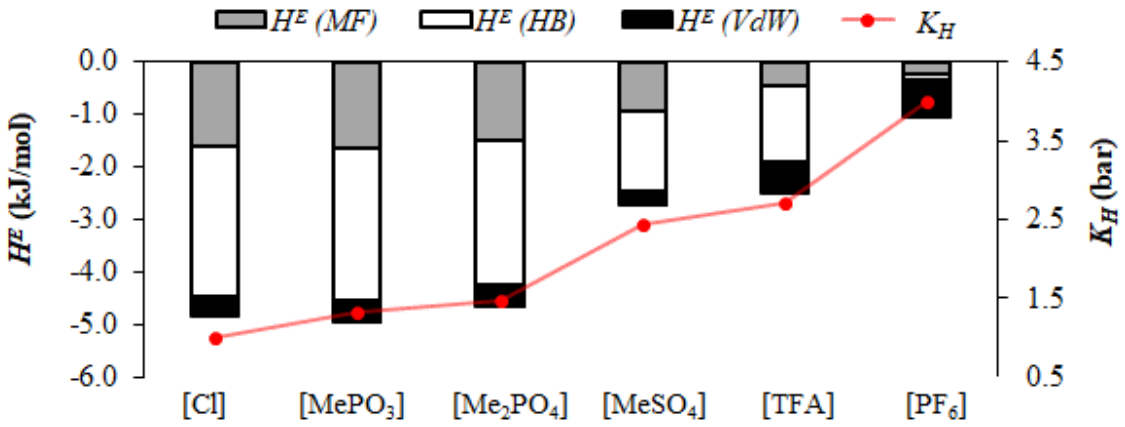

Figure 5: Excess Enthalpies (H^E) contributions (MF, HB and vdW) and Henry's law constants (K_H) of H_2S with different anions nature with the same cation $[emim]^+$

It is also analyzed the effect of different alkyl chains with the same anion ($[(Me)_2PO_4]^-$). Figure 6 presents the contributions to excess enthalpy and K_H as a function of the alkyl chain of the methylimidazolium based cation. As can be seen, the cation nature also affects the H_2S solubility in the IL, but with less influence than that of the anion. In all studied cases, the hydrogen bonding interactions present the higher contribution, being almost 68% of the total. The exothermic behavior of mixture is related to favorable solute-solvent interactions. ILs formed by methylimidazolium based cations with short alkyl chains present slightly better performance in the H_2S absorption, since the attractive electrostatic interactions are more effective when using shorter alkyl chains.

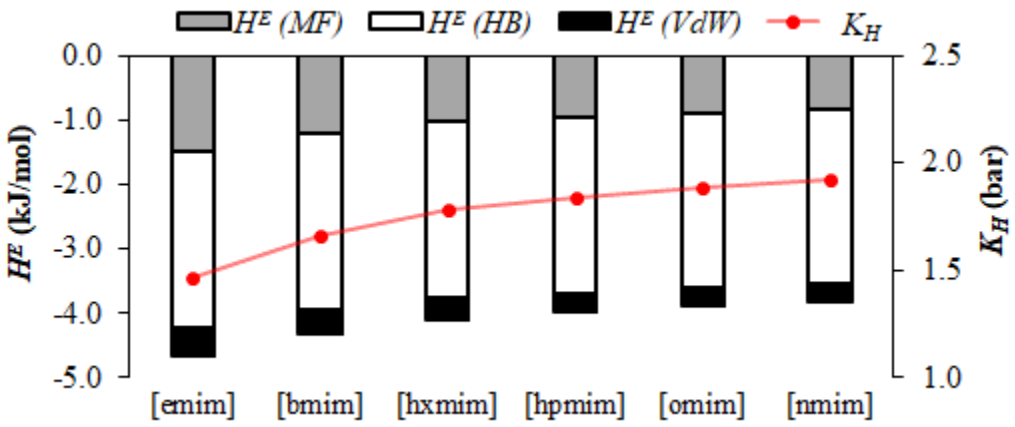

Figure 6: Excess Enthalpies *(H^E)* contributions (MF, HB and vdW) and Henry's law constants *(K_H)* of H_2S in different imidazolium based cations with the same anion $[(Me)_2PO_4]^-$

The last effect is shown in Figure 7 presenting the results of all the contributions to excess enthalpies and K_H of H_2S in different ILs presenting the same anion $[MePO_3]^-$, but varying the head group of the cation. As in previous analysis, the main contribution to the H_2S-IL mixing behavior is the hydrogen bond interactions (HB), representing a 70% of the total excess enthalpy value. ILs with cations presenting hydrogen-bond donor groups (as imidazolium or pyrrolidinium) present lower H_2S gas solubility, due to the competition between hydrogen-bond interactions of cation and anion and H_2S–anion interactions, as it was observed with other solutes [36, 40, 50]. In sum, current COSMO-RS results reveal that both anion and cation present great influence in the behavior of H_2S-IL mixtures. For the following process simulation analysis in this work, we selected 3 ILs that present favorable thermodynamic properties ([emim][$MePO_3$], [bmim][TFA] and [emim][$OcSO_4$]) from COSMO-RS analysis. In addition, we selected three ILs

([emim][DCN], [emim][SCN] and [emim][NTf_2]) that present worse thermodynamic behavior but lower viscosities and thus better expected transport properties [33].

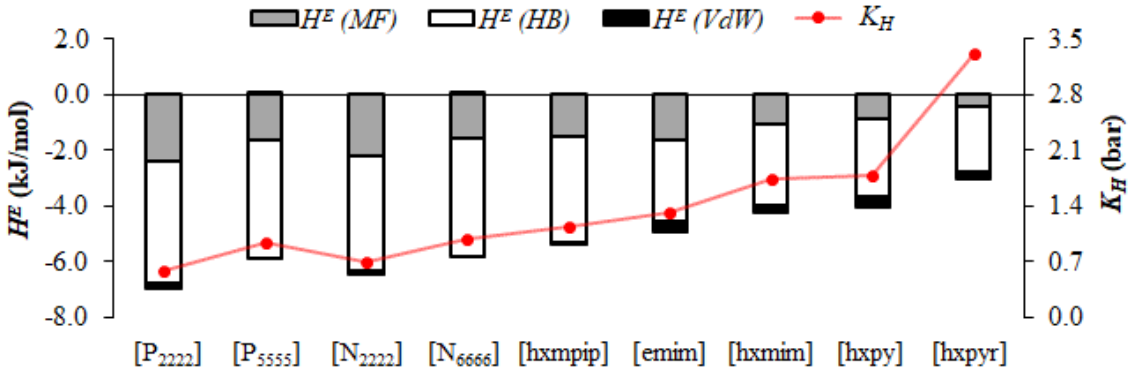

Figure 7: Excess Enthalpies *(H^E)* contributions (MF, HB and vdW) and Henry's law constants *(K_H)* of H_2S with different cations nature with the same anion $[MePO_3]^-$

Process Simulation Analysis

As first stage, COSMO-based/Aspen methodology was validated for the prediction gas-liquid equilibria data of H_2S-IL mixtures by comparing to available experimental data. Table 3 collects the mean relative errors of the gas-liquid equilibria (eq. 3) of four different ILs using the three COSMOSAC models commented in the methodology section. The experimental and calculated gas-liquid equilibria (GLE) data used to calculate these errors are collected in Figure S1 of the Supplementary Material. All the models describe reasonably well the GLE behavior of the mixture, presenting relative error < 30%. COSMOSAC 1 property model shows the best fit to the experimental data, with errors lower than 16%. This low dispersion can be considered an admissible error on initial stages of conceptual engineering of new processes based on ILs [28]. Therefore, COSMOSAC 1 is selected as the property model for next stages of the work.

Table 3: Mean relative errors of calculated solubilities using the different COSMOSAC property models, at temperatures between 30-80 ºC

IL	**[omim][PF_6]**	**[emim][NTf_2]**	**[hxmim][NTf_2]**	**[omim][NTf_2]**
Reference	[51]	[49]	[48]	[48]
P range (MPa)	0.12-1.92	0.16-1.61	0.11-2.02	0.13-1.69
COSMOSAC model	**Relative Error (%)**			
1	15.3	16.0	14.3	8.5
2	22.5	27.2	27.7	15.3
3	16.1	18.7	16.4	9.1

Once COSMO-based/Aspen approach was validated, different process simulations were carried out to systematically evaluate the performance of the selected ILs in H_2S absorption from a typical acid gas natural stream (Table 1), attending to the four cases detailed in Table 2.

Case 1: The performance of the selected ILs was first evaluated by modeling the absorption column in *Equilibrium* mode at a given number of stages and operating temperature. Figure 8 presents the achieved H_2S recovery when using the 6 different ILs with increasing liquid mass flow at two operating pressures (3 and 30 atm).

It is clear shown the advantage of using [emim][$MePO_3$] from the thermodynamic point of view, due to the lower *L/G* ratios required to reach high H_2S recoveries when compared to the other ILs. Comparing the two operation pressures (3 to 30 atm), it can be seen that a higher operating pressure allows using lower *L/G* ratios to reach the same H_2S recovery. [emim][$MePO_3$] presents the best thermodynamic behavior at both pressures. The overall process analysis suggests that H_2S absorption by ILs is not impeded from the thermodynamic point of view, reaching at 30 atm high solute recoveries with *L/G* ratios in the industrial range [52].

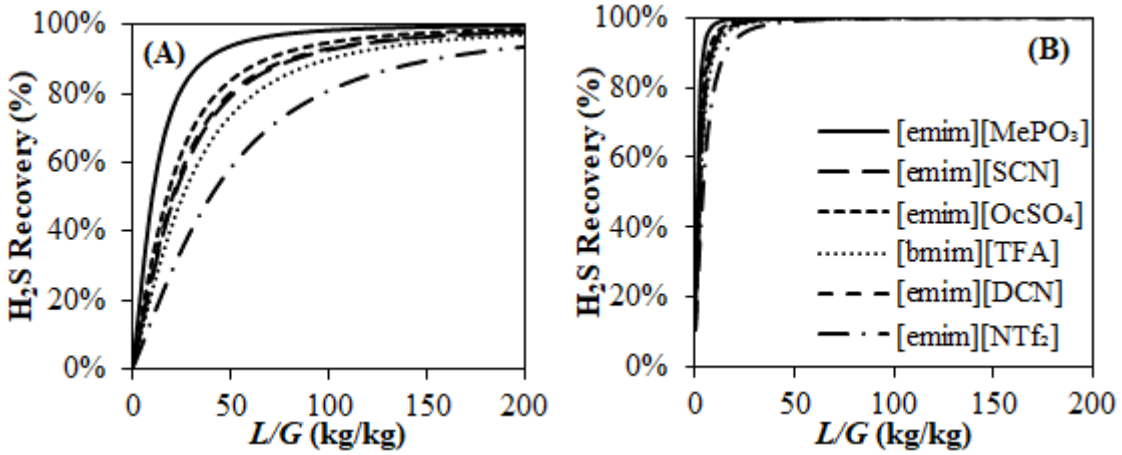

Figure 8: H_2S recoveries as a function of the *L/G* ratio at **(A)** 3 atm and **(B)** 30 atm (*Case 1* in Table 2)

Case 2: The aim of this study is to analyze the effect of the number of equilibrium stages of the absorption column in H_2S separation. Figure 9 presents the calculated number of stages required for reaching a H_2S recovery of 99% when using different *L/G* ratio for the selected ILs. As can be seen, from equilibrium-based simulations, it is possible to obtain high H_2S recoveries in a wide range of *L/G* and N_{stages} design variables. As expected, increasing the number of stages in the absorption column decreases the IL mass flow

required to achieve 99% of recovery. However, when increasing more than 5 stages, the required *L/G* ratio decreases in less proportion, converging into the same value. The shaded zone of the graph is referred to the work range (3 – 5 stages) more usually employed. This range was selected taking into account the heuristic value of 1 – 1.5 of *L/G* minimum for the separation [53]. For next stages, it was decided to work with an absorption column of 5 stages.

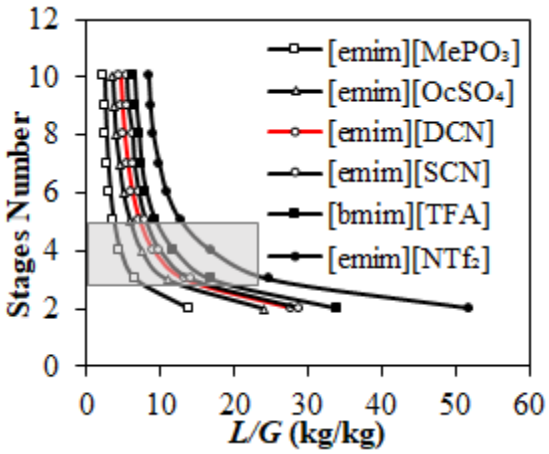

Figure 9: Stages number vs *L/G* ratio needed to reach a 99% H_2S recovery, using different ILs at 30 atm of pressure (*Case 2* in Table 2)

Case 3: This case of study introduces the mass transfer kinetics in the description of the absorption operation by using RADFRAC column in Rate-based mode. Thus, a more realistic scenario is studied, considering the transport properties of the mixture to estimate the H_2S separation efficiency by ILs in commercial packed columns. Figure 10 compares the H_2S recovery as a function of the absorption temperature using RADFRAC column in *Equilibrium* and *Rate-Based* modes with [emim][$MePO_3$] and [emim][DCN] ILs as absorbers. Simulations based on equilibrium show curves that follow the expected trends from exclusively thermodynamic consideration, *i.e.* the H_2S recovery increases when temperature decreases for both ILs, due to the higher gas solubility. In contrast, when absorption rate is considered in calculations, very low H_2S separation recovery was obtained for [emim][$MePO_3$] at near room temperature, as it was already observed when analyzing CO_2 capture by physical absorption with ILs [31, 33]. The results observed in Figure 10A reveal a strong kinetic control in the H_2S absorption phenomena in [emim][$MePO_3$] when using a commercial packed column at relatively low temperatures, assignable to the high viscosity of IL [31, 33]. Then, when increasing the operating temperature, the diffusivity of H_2S in IL is progressively enhanced, as consequence of the decreased IL viscosity [54], obtaining a maximum of H_2S recovery curve at 120 ºC, then

thermodynamics start to control the absorption process. Similar results are obtained for [emim][DCN] (Figure 10B), but with less remarkable differences between *Equilibrium* and *Rate-Based* mode due to the much lower viscosity of [emim][DCN] (16.83 cP @ 25 ºC [55]) when compared to [emim][$MePO_3$] (149.12 cP @ 25 ºC [56]).

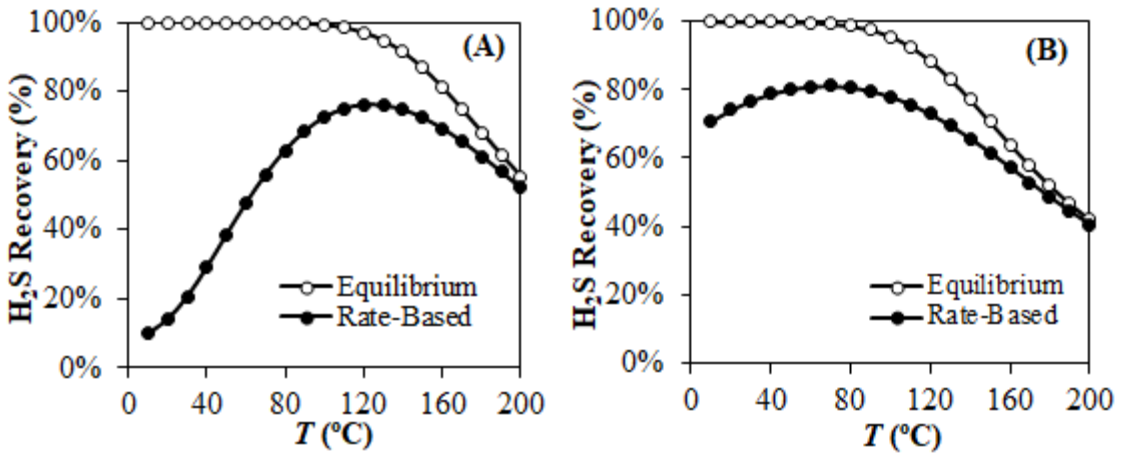

Figure 10: Comparative of the different H_2S recoveries as a function of the absorption temperature in both *Equilibrium* and *Rate-Based* modes of **(A)** [emim][$MePO_3$] and **(B)** [emim][DCN] (*Case 3* in Table 2)

Figure 11 completes current analysis, presenting the obtained H_2S recovery for all selected ILs when rigorous *Rate-based* absorption column model was used in simulations at different operating temperatures (25-200 ºC). The curves pass through a maximum in all cases, but at different temperature depending on the IL. Thus, [emim][DCN], [emim][SCN] and [emim][NTf_2] allow obtaining the maximum H_2S recovery at lower operating temperatures than those of [emim][$MePO_3$], [emim][$OcSO_4$] and [emim][TFA]. This may be explained by the lower viscosities of the first IL group compared to those of the second one [54]. In fact, at near room temperatures, the H_2S absorbent performance follows the trend of the IL viscosity values, which confirms that the mass transfer rate is controlling the H_2S absorption process in the column. On the contrary, at higher operating temperatures (than that corresponding to curve maximum) the absorption separation is determined by the thermodynamics of the H_2S-IL mixture (as in Figure 9). Based on current results, it is concluded that the IL [emim][DCN] operating at an absorption temperature of 50 ºC presents the best performance as H_2S absorbent.

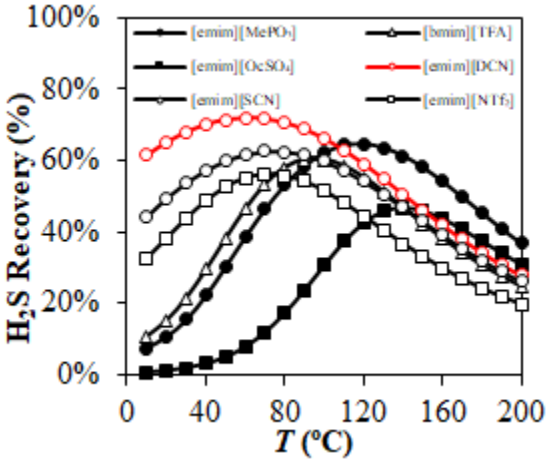

Figure 11: H_2S recoveries of the different ILs as a function of the absorption temperature (*Case 3* in Table 2)

Case 4. Finally, simulations to estimate the solvent consumption required to reach 95% of H_2S recovery at fixed operating conditions (see Table 2) were carried out for the selected ILs. Figure 12 presents the calculated *L/G* ratios needed to achieve this separation at different temperatures by using *Equilibrium* (only thermodynamic equilibrium is considered) and *Rate-Based* mode (mass transfer kinetic is also taken into account).

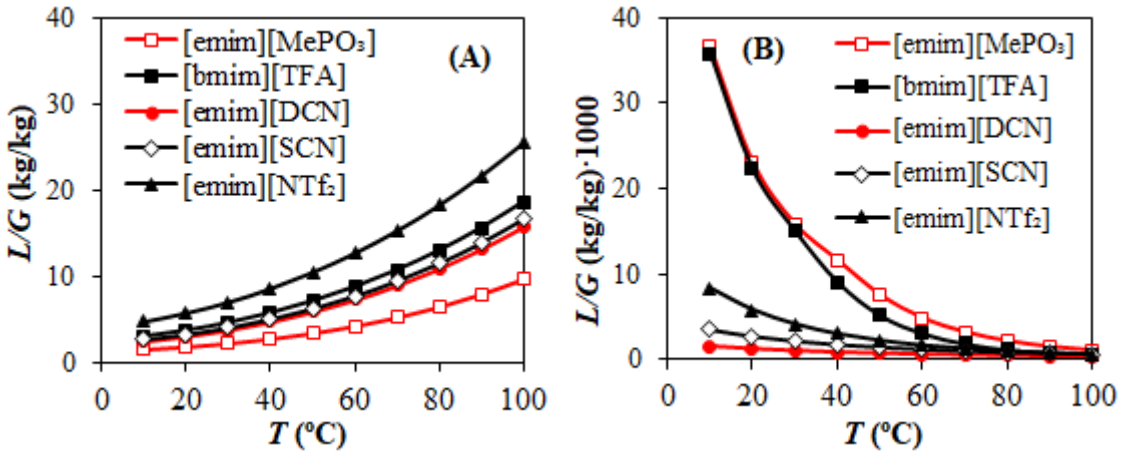

Figure 12: *L/G* mass ratio needed to reach a 95% of H_2S recovery at different temperatures for each IL using the RADFRAC model in **(A)** *Equilibrium* and **(B)** *Rate-Based* mode *(*Case 4 *in Table 2)*

As can be seen, huge differences are obtained when using the two different simulation approaches (*Equilibrium* or *Rate-Based* mode). Attending to Figure 12A, all the ILs present the same trend with absorption temperature, increasing IL mass flows by increasing temperatures, due to the lower H_2S gas solubility. In this case, the IL that presents the most favorable thermodynamic behavior is [emim][$MePO_3$]. In contrast, Figure 12B shows opposite trends of required *L/G* when increasing the operating

absorption temperature. In this case, the IL solvent expenses are higher at low temperatures due to the increasing IL viscosities [33]. In fact, the curves in Figure 12B follow an exponential decrease in good agreement with the dependence of viscosity values with temperature [54]. Again, it is observed that the IL [emim][DCN] presents the less viscous solvent. It is also important to remark the much higher *L/G* ratio needed (1000 time higher) when the mass transfer kinetics is taken into account in separation simulations at near room temperatures.

Absorption column design

Based on above results, the last purpose of the analysis is to design an H_2S absorption operation using [emim][DCN] at 50 ºC and 30 atm, to obtain a H_2S recovery of 95%. Figure 13 presents the required height (*H*) and diameter (*D*) of the packed column as a function of the *L/G* ratio. As can be seen, the use of a higher *L/G* ratio entails smaller column heights. On the other hand, an increase in the liquid mass flow demands larger column diameters for maintaining the fixed fractional capacity of 65%. The grey region corresponds to the design zone in which all the heuristic parameters are satisfied. In this sense, the height/diameter ratio in industrial absorption columns is between 3-15 [45] so different absorption columns with [emim][DCN] are possible. Thus, this study confirms the viability of [emim][DCN] IL to be used as absorbent of H_2S in gas streams in real applications. Future works with detailed cost estimations will be needed in order to optimize the design variables of H_2S absorption process based on ILs and compare their behavior with that of conventional absorbents.

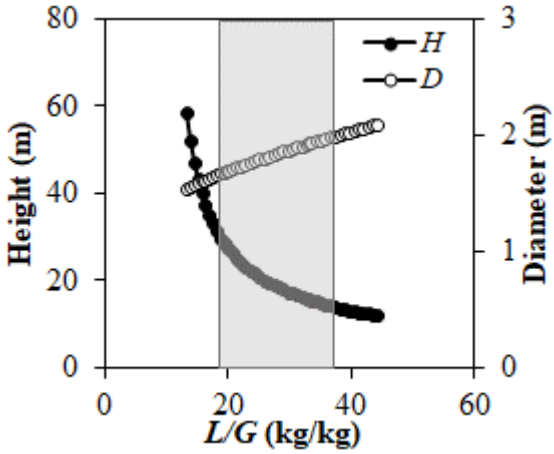

Figure 13: Absorption column design using [emim][DCN] as absorbent

Conclusions

In the present work, the modeling of H_2S absorption operation using ILs was accomplished. For this, a COSMO-based/Aspen Plus multiscale methodology was used. This methodology allows the *a priori* evaluation of the thermodynamic properties of a huge number of H_2S-IL mixtures. First, COSMOtherm molecular simulator was successfully applied to select different ILs among more than 700 attending to thermodynamic criteria (Henry's law constants). The results showed that it is expected a high H_2S solubility in some ILs due to the low K_H obtained. In addition, it was clear that the selection of the anion would have a great influence in the solubility, being favored with ions of hydrogen-bond acceptor character. The intermolecular interactions analysis remarks the high contribution on hydrogen bonding between H_2S solute and IL anion, traducing this into more exothermic mixtures. Second, Aspen Plus process simulator was used to test the H_2S solvent performance of selected ILs in absorption column. Despite the fact that no thermodynamic restrictions to H_2S separation were found (equilibrium-based recoveries of more than 99%), the strong kinetic control of the operation was determinant for the selection of both the operation conditions and the IL used. In this sense, the IL that shows the best thermodynamic behavior presents severe limited transport properties, implying very low H_2S recovery at near room temperatures. The IL that presents the best performance as H_2S absorbent is [emim][DCN], mainly due to its low viscosity, and thus improved transport properties. The operation temperature is the key parameter of the column design; being 50 ºC the one selected in which the recovery curve reaches the maximum absorption capacity. Lastly, the column design was accomplished with different design proposals, confirming the technical viability of the operation. Therefore, integrated molecular (COSMO-RS) and process (Aspen Plus) simulations analysis have been proved as a useful tool to achieve a prospective analysis of the potential application of ILs in the H_2S capture, providing a key comprehension on the IL selection and its application in a commercial absorption column before required experimental tests.

Acknowledgments

The authors thank Comunidad Autónoma de Madrid (Project P2018/EMT4348) and Ministerio de Economía y Competitividad (MINECO) of Spain (Project CTQ2017-

89441-R) for financial support. We are very grateful to Centro de Computación Científica de la Universidad Autónoma de Madrid for computational facilities.

References

1. British Petroleum, *Statistical review of world energy*. 2018.
2. Faramawy, S., T. Zaki, and A.A.E. Sakr, *Natural gas origin, composition, and processing: A review.* Journal of Natural Gas Science and Engineering, 2016. **34**: p. 34-54.
3. Astaria, G., D.W. Savage, and A. Bisio, *Gas treating with chemical solvents*. 1983: J. Wiley and Sons,New York, NY; None. Medium: X; Size: Pages: 493.
4. Ozekmekci, M., G. Salkic, and M.F. Fellah, *Use of zeolites for the removal of H_2S: A mini-review.* Fuel Processing Technology, 2015. **139**: p. 49-60.
5. Peters, L., et al., *CO_2 removal from natural gas by employing amine absorption and membrane technology—A technical and economical analysis.* Chemical Engineering Journal, 2011. **172**(2): p. 952-960.
6. Sigot, L., G. Ducom, and P. Germain, *Adsorption of hydrogen sulfide (H_2S) on zeolite (Z): Retention mechanism.* Chemical Engineering Journal, 2016. **287**: p. 47-53.
7. Zhou, L., et al., *Feasibility study on pressure swing sorption for removing H_2S from natural gas*. Vol. 59. 2004. 2401-2406.
8. Kidnay, A.J. and W.R. Parrish, *Fundamentals of Natural Gas Processing*. 2006: CRC Press.
9. Mandal, B.P., A.K. Biswas, and S.S. Bandyopadhyay, *Selective absorption of H_2S from gas streams containing H_2S and CO_2 into aqueous solutions of N-methyldiethanolamine and 2-amino-2-methyl-1-propanol.* Separation and Purification Technology, 2004. **35**(3): p. 191-202.
10. Lu, J.-G., Y.-F. Zheng, and D.-L. He, *Selective absorption of H_2S from gas mixtures into aqueous solutions of blended amines of methyldiethanolamine and 2-tertiarybutylamino-2-ethoxyethanol in a packed column.* Separation and Purification Technology, 2006. **52**(2): p. 209-217.
11. Bara, J.E., *Potential for Hydrogen Sulfide Removal Using Ionic Liquid Solvents*, in *Green Solvents II: Properties and Applications of Ionic Liquids*, A. Mohammad and D. Inamuddin, Editors. 2012, Springer Netherlands: Dordrecht. p. 155-167.
12. Burr, B. and L. Lyddon, *A Comparison of Physical Solvents for Acid Gas Removal*. Vol. 1. 2008.
13. Wilkes, J.S., P. Wasserscheid, and T. Welton, *Ionic Liquids in Synthesis*. 2008: Wiley-VCH Verlag GmbH & Co. KGaA. 1-6.
14. Welton, T., *Ionic liquids: a brief history.* Biophysical Reviews, 2018. **10**(3): p. 691-706.
15. Shang, D., et al., *Ionic liquids in gas separation processing.* Current Opinion in Green and Sustainable Chemistry, 2017. **5**: p. 74-81.
16. Jou, F.-Y. and A.E. Mather, *Solubility of Hydrogen Sulfide in [bmim][PF_6].* International Journal of Thermophysics, 2007. **28**(2): p. 490.
17. Jalili, A.H., et al., *Solubility of H_2S in Ionic Liquids [bmim][PF_6], [bmim][BF_4], and [bmim][Tf_2N].* Journal of Chemical & Engineering Data, 2009. **54**(6): p. 1844-1849.

18. Jalili, A.H., et al., *Solubility and diffusion of CO_2 and H_2S in the ionic liquid 1-ethyl-3-methylimidazolium ethylsulfate.* The Journal of Chemical Thermodynamics, 2010. **42**(10): p. 1298-1303.
19. Shiflett, M.B., A.M.S. Niehaus, and A. Yokozeki, *Separation of CO_2 and H_2S Using Room-Temperature Ionic Liquid [bmim][$MeSO_4$].* Journal of Chemical & Engineering Data, 2010. **55**(11): p. 4785-4793.
20. Zhao, Y., et al., *Hydrogen Sulfide Solubility in Ionic Liquids (ILs): An Extensive Database and a New ELM Model Mainly Established by Imidazolium-Based ILs.* Journal of Chemical & Engineering Data, 2016. **61**(12): p. 3970-3978.
21. Pomelli, C.S., et al., *Influence of the Interaction between Hydrogen Sulfide and Ionic Liquids on Solubility: Experimental and Theoretical Investigation.* The Journal of Physical Chemistry B, 2007. **111**(45): p. 13014-13019.
22. Aparicio, S. and M. Atilhan, *Computational Study of Hexamethylguanidinium Lactate Ionic Liquid: A Candidate for Natural Gas Sweetening.* Energy & Fuels, 2010. **24**(9): p. 4989-5001.
23. Sakhaeinia, H., et al., *Solubility of H_2S in 1-(2-hydroxyethyl)-3-methylimidazolium ionic liquids with different anions.* Fluid Phase Equilibria, 2010. **298**(2): p. 303-309.
24. Zhao, Y., et al., *Predicting H_2S solubility in ionic liquids by the quantitative structure-property relationship method using S sigma-profile molecular descriptors.* Rsc Advances, 2016. **6**(74): p. 70405-70413.
25. Kamgar, A. and F. Esmaeilzadeh, *Prediction of H_2S solubility in hmim Pf(6) , hmim Bf(4) and hmim Tf_2N using UNIQUAC, NRTL and COSMO-RS.* Journal of Molecular Liquids, 2016. **220**: p. 631-634.
26. Mortazavi-Manesh, S., M.A. Satyro, and R.A. Marriott, *Screening ionic liquids as candidates for separation of acid gases: Solubility of hydrogen sulfide, methane, and ethane.* Aiche Journal, 2013. **59**(8): p. 2993-3005.
27. Santiago, R., et al., *Acetylene absorption by ionic liquids: A multiscale analysis based on molecular and process simulation.* Separation and Purification Technology, 2018. **204**: p. 38-48.
28. Ferro, V.R., et al., *Enterprise Ionic Liquids Database (ILUAM) for Use in Aspen ONE Programs Suite with COSMO-Based Property Methods.* Industrial & Engineering Chemistry Research, 2018. **57**(3): p. 980-989.
29. Ferro, V.R., et al., *Introducing process simulation in ionic liquids design/selection for separation processes based on operational and economic criteria through the example of their regeneration.* Separation and Purification Technology, 2012. **97**: p. 195-204.
30. De Riva, J., et al., *Aspen Plus supported analysis of the post-combustion CO2 capture by chemical absorption using the [P_{2228}][CNPyr] and [P_{66614}][CNPyr] AHA Ionic Liquids.* International Journal of Greenhouse Gas Control, 2018. **78**: p. 94-102.
31. de Riva, J., et al., *Ionic liquids for post-combustion CO_2 capture by physical absorption: Thermodynamic, kinetic and process analysis.* International Journal of Greenhouse Gas Control, 2017. **61**: p. 61-70.
32. Palomar, J., et al., *Understanding the Physical Absorption of CO_2 in Ionic Liquids Using the COSMO-RS Method.* Industrial & Engineering Chemistry Research, 2011. **50**(6): p. 3452-3463.
33. Palomar, J., et al., *Demonstrating the key role of kinetics over thermodynamics in the selection of ionic liquids for CO_2 physical absorption.* Separation and Purification Technology, 2019. **213**: p. 578-586.

34. Palomar, J., et al., *Task-specific ionic liquids for efficient ammonia absorption.* Separation and Purification Technology, 2011. **82**: p. 43-52.
35. Bedia, J., et al., *Optimized ionic liquids for toluene absorption.* Aiche Journal, 2013. **59**(5): p. 1648-1656.
36. Gonzalez-Miquel, M., J. Palomar, and F. Rodriguez, *Selection of Ionic Liquids for Enhancing the Gas Solubility of Volatile Organic Compounds.* The Journal of Physical Chemistry B, 2013. **117**(1): p. 296-306.
37. Fallanza, M., et al., *Screening of RTILs for propane/propylene separation using COSMO-RS methodology.* Chemical Engineering Journal, 2013. **220**: p. 284-293.
38. Liu, X., et al., *High Solubilities for Methane, Ethane, Ethylene, and Propane in Trimethyloctylphosphonium Bis(2,4,4-trimethylpentyl) Phosphinate ([P_{8111}][TMPP]).* Industrial & Engineering Chemistry Research, 2014. **53**(1): p. 363-368.
39. de Riva, J., et al., *Aspen Plus supported conceptual design of the aromatic–aliphatic separation from low aromatic content naphtha using 4-methyl-N-butylpyridinium tetrafluoroborate ionic liquid.* Fuel Processing Technology, 2016. **146**: p. 29-38.
40. Moreno, D., et al., *Absorption refrigeration cycles based on ionic liquids: Refrigerant/absorbent selection by thermodynamic and process analysis.* Applied Energy, 2018. **213**: p. 179-194.
41. Stull, D.R., *Vapor Pressure of Pure Substances. Organic and Inorganic Compounds.* Industrial & Engineering Chemistry, 1947. **39**(4): p. 517-540.
42. Lin, S.-T. and S.I. Sandler, *A Priori Phase Equilibrium Prediction from a Segment Contribution Solvation Model.* Industrial & Engineering Chemistry Research, 2002. **41**(5): p. 899-913.
43. Klamt, A., *Conductor-like Screening Model for Real Solvents: A New Approach to the Quantitative Calculation of Solvation Phenomena.* The Journal of Physical Chemistry, 1995. **99**(7): p. 2224-2235.
44. S.-T. Lin, P.M.M., Y. Song, C.-C. Chen, and S. I. Sandler, *Improvements of Phase-Equilibrium Predictions for Hydrogen-Bonding Systems from a New Expression for COSMO Solvation Models*, in *AIChE Annual Meeting*. 2002: Indianapolis.
45. Ulrich, G.D., *Chemical Engineering Process Design and Economics: A Practical Guide*. 2004: Process Publishing.
46. Klamt, A., F. Eckert, and W. Arlt, *COSMO-RS: An Alternative to Simulation for Calculating Thermodynamic Properties of Liquid Mixtures.* Annual Review of Chemical and Biomolecular Engineering, 2010. **1**(1): p. 101-122.
47. Ruiz, E., et al., *Evaluation of ionic liquids as absorbents for ammonia absorption refrigeration cycles using COSMO-based process simulations.* Applied Energy, 2014. **123**: p. 281-291.
48. Jalili, A.H., et al., *Solubility of CO_2, H_2S, and Their Mixture in the Ionic Liquid 1-Octyl-3-methylimidazolium Bis(trifluoromethyl)sulfonylimide.* The Journal of Physical Chemistry B, 2012. **116**(9): p. 2758-2774.
49. Sakhaeinia, H., et al., *Solubility of H_2S in Ionic Liquids 1-Ethyl-3-methylimidazolium Hexafluorophosphate ([emim][PF_6]) and 1-Ethyl-3-methylimidazolium Bis(trifluoromethyl)sulfonylimide ([emim][Tf_2N]).* Journal of Chemical & Engineering Data, 2010. **55**(12): p. 5839-5845.
50. Ruiz, E., et al., *Interactions of Ionic Liquids and Acetone: Thermodynamic Properties, Quantum-Chemical Calculations, and NMR Analysis.* The Journal of Physical Chemistry B, 2013. **117**(24): p. 7388-7398.

51. Safavi, M., et al., *Study of the solubility of CO_2, H_2S and their mixture in the ionic liquid 1-octyl-3-methylimidazolium hexafluorophosphate: Experimental and modelling.* The Journal of Chemical Thermodynamics, 2013. **65**: p. 220-232.
52. Azizi, M., et al., *Simulation of hydrogen sulphide absorption in alkaline solution using a packed column*. Vol. 35. 2014. 3105-3115.
53. Sinnott, R.K., *Chapter 11 - Separation Columns (Distillation and Absorption)*, in *Coulson and Richardson's Chemical Engineering (Second Edition)*, R.K. Sinnott, Editor. 1993, Pergamon: Amsterdam. p. 439-564.
54. de Riva, J., et al., *Statistical Refinement and Fitting of Experimental Viscosity-to-Temperature Data in Ionic Liquids.* Industrial & Engineering Chemistry Research, 2014. **53**(25): p. 10475-10484.
55. Neves, C.M.S.S., et al., *Systematic Study of the Thermophysical Properties of Imidazolium-Based Ionic Liquids with Cyano-Functionalized Anions.* The Journal of Physical Chemistry B, 2013. **117**(35): p. 10271-10283.
56. Hiraga, Y., et al., *Densities at Pressures up to 200 MPa and Atmospheric Pressure Viscosities of Ionic Liquids 1-Ethyl-3-methylimidazolium Methylphosphate, 1-Ethyl-3-methylimidazolium Diethylphosphate, 1-Butyl-3-methylimidazolium Acetate, and 1-Butyl-3-methylimidazolium Bis(trifluoromethylsulfonyl)imide.* Journal of Chemical & Engineering Data, 2015. **60**(3): p. 876-885.